*Molecular Medicine in Practice*

# Exon 11 Skipping of E-Cadherin RNA Downregulates Its Expression in Head and Neck Cancer Cells

Sanjai Sharma[1], Wei Liao[1], Xiaofeng Zhou[2], David T.W. Wong[3], and Alan Lichtenstein[1]

## Abstract

*E-cadherin* is an important tumor suppressor gene whose expression is lost when cells acquire a metastatic phenotype. We analyzed the role of E-cadherin missplicing as a mechanism of its downregulation by analyzing a misspliced E-cadherin transcript that lacks exon 11 of this gene. This results in a frameshift and a premature termination codon that targets this transcript for degradation. Tumor tissues, including breast (20%, $n = 9$), prostate (30%, $n = 9$) and head and neck (75%, $n = 8$) cancer, express the exon 11-skipped transcripts (vs. nonmalignant controls) and its levels inversely correlate with E-cadherin expression. This is a novel mechanism of E-cadherin downregulation by missplicing in tumor cells, which is observed in highly prevalent human tumors. In the head and neck cancer model, nontumorigenic keratinocytes express exon 11–skipped splice product two- to sixfold lower than the head and neck tumor cell lines. Mechanistic studies reveal that SFRS2 (SC35), a splicing factor, as one of the regulators that increases missplicing and downregulates E-cadherin expression. Furthermore, this splicing factor was found to be overexpressed in 5 of 7 head and neck cell lines and primary head and neck tumors. Also, methylation of E-cadherin gene acts as a regulator of this aberrant splicing process. In 2 head and neck cell lines, wild-type transcript expression increased 16- to 25-folds, whereas the percentage of exon 11-skipped transcripts in both the cell lines decreased five- to 30-folds when cells were treated with a hypomethylating agent, azacytidine. Our findings reveal that promoter methylation and an upregulated splicing factor (SFRS2) are involved in the E-cadherin missplicing in tumors. *Mol Cancer Ther; 10(9); 1751–9. ©2011 AACR.*

## Introduction

Presence of a premature termination (PTC) codon mutation results in an in-frame stop codon in RNA. These RNA transcripts are degraded by pathway called the nonsense-mediated decay (NMD) pathway that is active in all mammalian cells (1–3). Theoretically, the NMD prevents expression of truncated proteins that could act as dominant negatives and have adverse effects. PTC in a RNA transcript could be because of a point mutation or a frameshift, and the rapid degradation of PTC-containing RNAs can be a mechanism by which loss-of-function of potential tumor suppressor genes can occur. Alternative splicing affects more than 60% of the human genes (4) and cancer cells are known to have different splicing patterns as compared with their normal counterparts (5). Cancer cells are also associated with alternative splicing of several tumor suppressors genes, such as *BRCA1/2*, *APC*, *WT1*, *mdm2*, and *ATM* (6–10) with subsequent NMD-mediated degradation and loss of expression.

Changes in splicing patterns in tumor cells could be secondary to aberrant expression of splice factors affecting the splicing patterns of a number of genes. Recent reports on aberrant expression of serine-arginine rich (SR) proteins, SFRS1 and SFRS2 splicing factors exemplify their potential role in transformation (11, 12). Splicing factors are also regulated by oncogenic signaling pathways that affect activity of SR proteins (13).

Methylation affects transcription of the gene (14) that in turn is intricately linked to splicing as both processes occur simultaneously (15, 16). As splicing factors are also known to associate with the transcriptional machinery (17), the nature of the transcriptional complex assembled for the transcription of a particular gene influences the splicing factors available for splicing which in turn affects the splicing patterns. Methylation changes can also occur at the lysine residues of the histones that are able to modify the chromatin structure, which are now recognized as important regulator of alternative splicing (18, 19), and in fact, define the exon–intron boundaries (20). The epigenetic events associated with methylation

**Authors' Affiliations:** [1]Division of Hematology Oncology, UCLA West Los Angeles VA Medical Center, West Los Angeles, California; [2]Center for Molecular Biology of Oral Diseases, UIC Cancer Center, College of Dentistry, University of Illinois at Chicago, Illinois; and [3]Dental Research Institute, School of Dentistry, University of California at Los Angeles, California

**Note:** Supplementary material for this article is available at Molecular Cancer Therapeutics Online (http://mct.aacrjournals.org/).

**Corresponding Author:** Sanjai Sharma, Division of Hematology Oncology, UCLA West Los Angeles VA Medical Center, 11301 Wilshire Blvd, Bldg 304, Rm E1-115, Los Angeles, CA 90073. Phone: 310-268-3247; Fax: 310-268-3190; E-mail: sasharma@mednet.ucla.edu

**doi:** 10.1158/1535-7163.MCT-11-0248

©2011 American Association for Cancer Research.

American Association for *Cancer Research*

could thereby potentially affect splicing with change in transcriptional rates and histone modifications.

We have previously reported an E-cadherin exon 11–skipped, alternatively spliced transcript that is subject to NMD degradation in chronic lymphocytic leukemia cells (21). This tumor suppressor gene has a critical role in maintaining cell–cell adhesion and cell–matrix interactions (reviewed in refs. 22, 23). As these functions are important for the epithelial membrane integrity, missplicing of this transcript was analyzed in epithelial cancers. We report the presence of this exon 11–skipped transcript in primary human cancer tissues and further characterize its regulation by splicing factors and methylation status of the *E-cadherin* gene.

## Materials and Methods

### Primary human tissues and TissueScan arrays

Primary human head and neck cancer specimens (8 matched pairs) and matched normal controls were obtained from the Cooperative Human Tissue Network. Tissue RNA was isolated by grinding frozen tissues in RLT buffer (Qiagen RNA Kit) followed by the kit isolation protocol. TissueScan quantitative PCR arrays for breast, prostate, and other cancers were purchased from Origene. Each tissue type has 9 individual tumor cDNA and 3 tissue-matched normals. Both primary human tissues and TissueScan arrays were analyzed by light microscopy to confirm the quality and the nature of the tissues.

### Transcript-specific real-time PCR

E-cadherin expression in cells was analyzed by a real-time PCR. The 5′-primer GGATGTGCTGGATGTGAATG localizes to exon 10 of the *E-cadherin* gene. The 3′-primer CACATCAGACAGGATCAGCAGAA localizes to the exon 12. The TaqMan probe 10–11 (TAACATATCG-GATTTGGAGAGAC) determining the wild-type E-cadherin transcript level binds to the junction of exon 10–exon 11. The expression level of the skipped or aberrant transcript (transcript lacking exon 11) is determined by the same set of PCR primers as mentioned above with a TaqMan probe 10–12 (CAGAAAATAACGTTCTCCAGTTG) binding the exon 10–exon 12 junction. Real-time PCR for actin expression was used as a control and relative expression of transcripts was determined by comparative $C_t$ method of Pfall (24) that compares transcript levels in different samples by using a coamplified internal control.

### Cell culture and microarray analysis

The head and neck cancer cell lines UMSCC1, 2, 12, 14, 22b were obtained from University of Michigan, Ann Arbor, MI. Cal27 was obtained from American Type Culture Collection. Telomerase reverse transcriptase immortalized keratinocytes (tert-kert) and normal human oral keratinocytes (NHOK) cells were obtained from Dr. David Wong's lab (UCLA Dental School) and cultured as previously described (25). No further authentication of the cell lines was done by the authors. Emetine treatment was

done at concentration of 100 μg/mL for 8 hours (10). In some groups, actinomycin D was added at a concentration of 2 μg/mL, together with emetine (100 μg/mL; ref. 26). For microarray analysis, cRNA was obtained as per standard protocols and hybridized to the Affymetrix chip 133A (Affymetrix). The nonsense transcript enrichment index (26) score is the ratio of upregulation of the signal intensity on emetine treatment of head and neck squamous cell carcinomas cells of a particular probe set divided by the ratio of upregulation of signal intensity of nonmalignant tert-kert cells for the same probe set.

### Minigene constructs

Exon 10, 11, and 15 of the E-cadherin gene along with their flanking intronic regions were cloned into a minigene construct pDup (gift from Dr. Douglas Black, UCLA; ref. 27). The exon 10 is 245 base pairs (bp) and a DNA fragment from position −325 from 5′-exon–intron junction to +338 from the 3′-exon–intron junction was amplified by PCR from normal human peripheral blood mononuclear cells DNA and cloned in the pDup vector at the Apa1 and BglII site. Similarly, for exon 11 (146 bp) a fragment −623 to +544 and for exon 15, a fragment from −477 to +518 was cloned. The constructs were transiently transfected in SCC12 cells and cells were analyzed by reverse transcriptase PCR (RT-PCR) analysis. The primers for amplification are GACACCATGCATGGTGCACC and GCAGCTCA-CTCAGTGTGGCA, which bind to β-globin exon E1 and E3, respectively. To quantify the amount of correctly or aberrantly spliced transcripts, a real-time PCR was conducted with TaqMan probes specifically binding the junction of β-globin E1–exon 11 or β-globin E1–β-globin E3. Cells were transfected with 1 μg of plasmid along with 5 μg of bluescript DNA and Lipofectamine 2000 (Invitrogen). Forty-eight hours after transfection, cells were analyzed by real-time RT-PCR.

### Analysis of splicing factors and short interfering RNA knockdown

Head and neck cell lines were analyzed for expression of splicing factors SFRS1, 2, 5, and 6 with real-time PCR (Applied Biosystems). The SCC12 and SCC1 lines were transfected with 10 nmol/L short interfering RNA (siRNA) and 1 μg of the minigene exon 11 construct siRNA against SFRS2 (Santa Cruz Biotechnology). Western blot analysis for SFRS2 expression was carried out with Santa Cruz Biotechnology antibody, E-16. Forty-eight hours after transfection, the cells were analyzed for SRFS2 expression and quantitative transcript–specific real-time PCR analysis for E-cadherin splicing.

### DNA hypomethylation

SCC1 and 22b cell lines were treated with 5-aza-deoxycytidine (5 μmol/L) for 96 hours and cells analyzed for E-cadherin RNA expression by transcript-specific real-time PCR. In parallel, DNA was isolated and bisulfite-modified methylation-specific PCR conducted as described (28), along with Western blot analysis for E-cadherin.

## Results
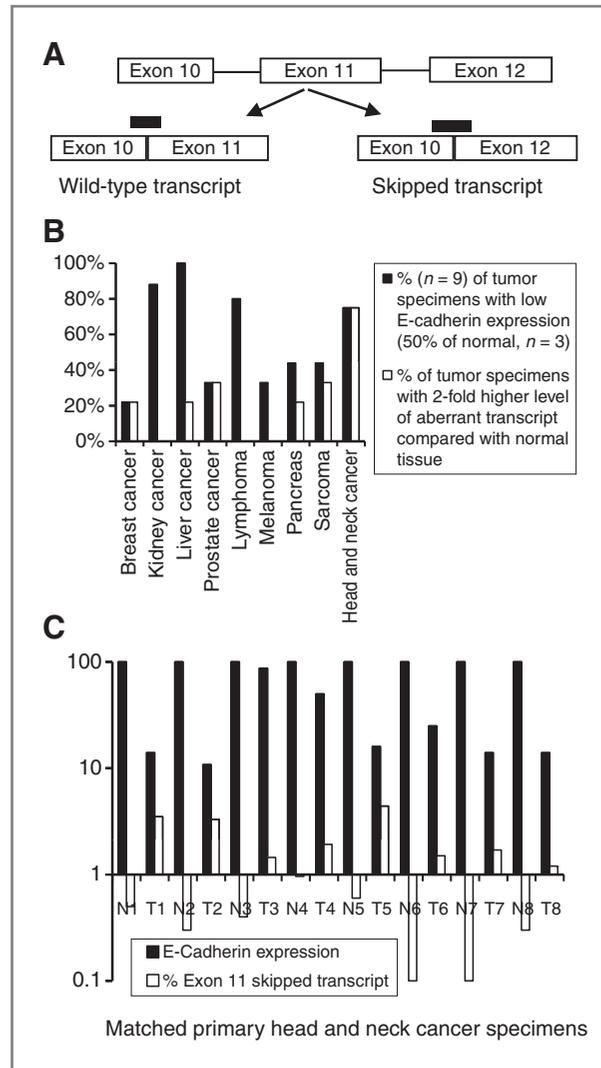
### Wild-type and exon 11–skipped transcript

To ascertain whether exon 11–skipped transcripts are present in solid tumors, we screened 8 pairs of head and neck cancer primary tissues (tumor and matched normal). For lymphomas, melanomas, sarcomas, breast, kidney, liver, pancreas prostate cancers, a tissue scan PCR array with 9 tumor cDNAs and 3 normal tissue cDNAs was analyzed. A transcript-specific real-time PCR was conducted on all tissues that distinguished normal wild-type transcripts from the exon 11–skipped transcripts (Fig. 1A).

Figure 1B shows percent of each tumor type with E-cadherin RNA expression, which is decreased, compared with corresponding control tissue (at least 50% expression decrease vs. nonmalignant control tissue, black bars). To estimate the relative abundance of the aberrant transcript as compared with the wild type in tissues, the difference between the $\Delta C_t$ of the transcript-specific PCR reactions was calculated by using the cycle difference in the 2 transcripts to calculate the relative abundance, for example, with 8 cycle difference between the 2 transcripts, the exon 11–skipped transcript is 0.4% of the wild type. The percent of each tumor type with at least a 2-fold higher level of exon 11–skipped transcript compared with corresponding normal tissue is shown in Fig. 1B (open bars). As shown in Fig. 1B, tumor types with the highest incidence of loss of normal E-cadherin RNA expression were kidney cancer (90%), liver cancer (100%), lymphoma (80%), and head and neck cancer (75%). Although the sample size in this screening is relatively small, these data are consistent with previous literature (29–31) that also identified loss of E-cadherin expression as being frequent in these cancers. Of these 4 tumor types, the one with the highest frequency of increased expression of exon 11–skipped transcripts was head and neck cancer (open bar, 7 of 9 specimens), and this tumor was chosen for further analysis.

Figure 1C depicts the results of the transcript-specific PCR assay for each head and neck cancer specimen. Relative amounts of wild-type RNA are shown in closed bars and percentage of exon 11–skipped transcripts in open bars (log scale). As can be seen, there is an inverse correlation between the relative amount of normal E-cadherin RNA expression and exon 11–skipped RNA ($P = 0.08$, correlative coefficient). It should be noted that this is an underestimation of the exon 11–skipped transcripts as the NMD pathway had been active in these cells, which would have caused constant rapid degradation of this transcript and not the wild type.

### Microarray analysis with inhibition of NMD pathway

An unbiased screen for PTC codons in 5 head and neck cancer cell lines (UMSCC1, 2, 12, 14, and 22b) also supported the frequency of a PTC-bearing transcript that was caused by exon 11 skipping. In this screen, the NMD pathway was paralyzed by a short exposure to emetine as previously described (26) and microarray



**Figure 1.** Aberrant transcripts in primary human tumor tissues. A, schematic showing the location of the probes to identify the wild-type and aberrant transcript (exon 11 skipped). B, different types of human cancer cDNA analyzed by real-time PCR analysis for wild-type and aberrant E-cadherin transcript ($n = 9$ for each tumor, $n = 3$ for matched organ-specific normal tissue). Black bars represent the percentage of tumor cDNAs with E-cadherin expression less than 50% of matched normal tissue; open bars represent the percentage of tumor cDNAs in which the percentage of aberrant transcript is at least 2-fold greater than the aberrant transcript in matched normal tissue. For the head and neck cancer group, the data show relative levels of total E-cadherin expression in 8 pairs of matched normal (N) and tumor tissues (T), relative to actin and adjusted to the matched normal control. C, head and neck cancer data from 8 matched groups is shown with wild type and percentage of exon 11–skipped transcript in each matched pair (log scale).

RNA profiling was done with or without NMD paralysis. Immortalized nontransformed tert-kert cells were used as control cell and compared with 5 head and neck cell lines (GEO accession number GSE29788). A more than 5-fold mean emetine-induced upregulation was observed in 199 of 23,000 probes. The initial hits (significant upregulations by emetine) were also analyzed

for RNA signal intensity versus tert keratinocytes in the absence of emetine. Our reasoning was that those with downregulated expression were most likely to represent loss-of-function tumor suppressors. The *E-cadherin* gene was identified as one of the top 100 maximally downregulated genes when comparing head and neck tumor lines to tert keratinocytes, and its RNA signal was significantly increased upon NMD paralysis with emetine (Supplementary Data).

To confirm these findings, we treated the head and neck line UMSCC14A with emetine to paralyze the NMD. As emetine exposure also results in upregulation of a number of stress response genes via stress-induced transcription, actinomycin D was added to block the upregulation of stress-induced transcription (32). Following exposure to emetine or emetine + actinomycin D, RT-PCR analysis was done (Fig. 2A). The primers for this PCR bind to the 3′ end of the *E-cadherin* gene, and a

stronger band was observed in the emetine-treated cells. Importantly, addition of actinomycin D did not prevent this upregulation, indicating the emetine-induced upregulation was not due to a stress response that activates transcription. Figure 2A shows a contrasting example of the fibroblast growth factor receptor substrate 2 (*FRS2*) gene for which the emetine-induced upregulation was prevented by addition of actinomycin D. Upon sequencing the entire cDNA of FRS2, no PTC mutations were identified. In contrast, sequencing showed that, in addition to the wild-type E-cadherin transcript, a smaller transcript was identified that lacked exon 11 and resulted in a frameshift and a PTC located in exon 12 as previously described (21).

### Half-life of the exon 11–skipped transcript

To further support the notion that the PTC-containing RNA is rapidly degraded by the NMD, we studied the
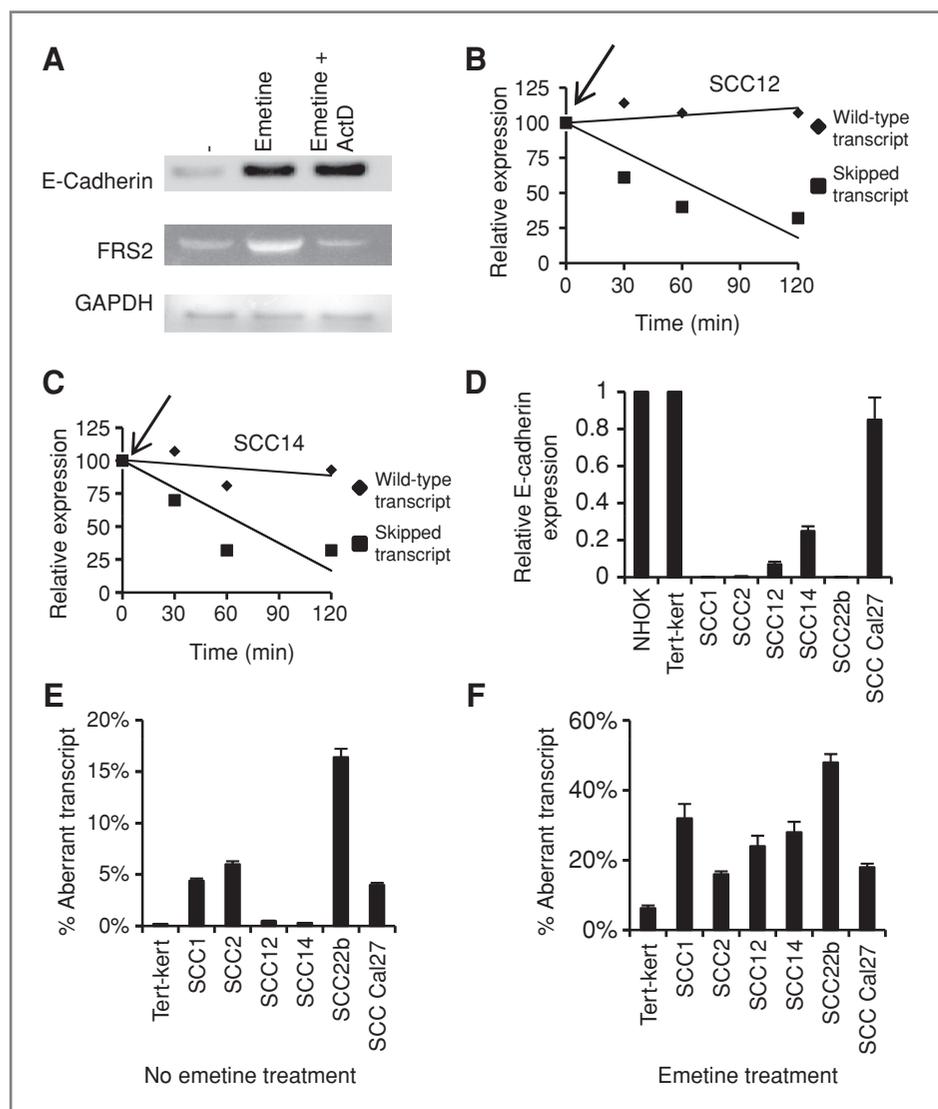


**Figure 2.** Analysis of the aberrant transcript. A, RT-PCR analysis of untreated UMSCC12 cells treated with emetine or emetine plus actinomycin-D and analyzed for expression of E-cadherin RNA. With the same cDNA preparation FRS2 and glyceraldehyde-3-phosphate dehydrogenase (GAPDH) were amplified. B and C, UMSCC14 and UMSCC12 cells were treated with actinomycin-D, and transcript-specific PCR conducted at different time points. D, relative expression of E-cadherin in tert keratinocytes, NHOK, and head and neck cell lines relative to expression in tert-kert cells. E, percentage exon 11–skipped transcript calculated by the cycle difference between the 2 transcripts with transcript-specific real-time PCR of untreated (E) and emetine treated, (F) cells.

**Figure 3.** Minigene experiments show similar splicing patterns. A, schematic showing the minigene constructs with E-cadherin exon 10, 11, and 15. B, transient transfection and RT-PCR analysis (DNA gel) of UMSCC12 cells transfected with various minigene constructs. Primers bind to β−globin exon E1 and E3. Upper arrow indicates the correct expected size and the lower arrow indicates a transcript lacking exon 11. C, schematic for the location of probes for transcript-specific PCR. D, real-time PCR data showing the percentage aberrant transcript in tert-kert and head and neck cell lines (mean ± SD).
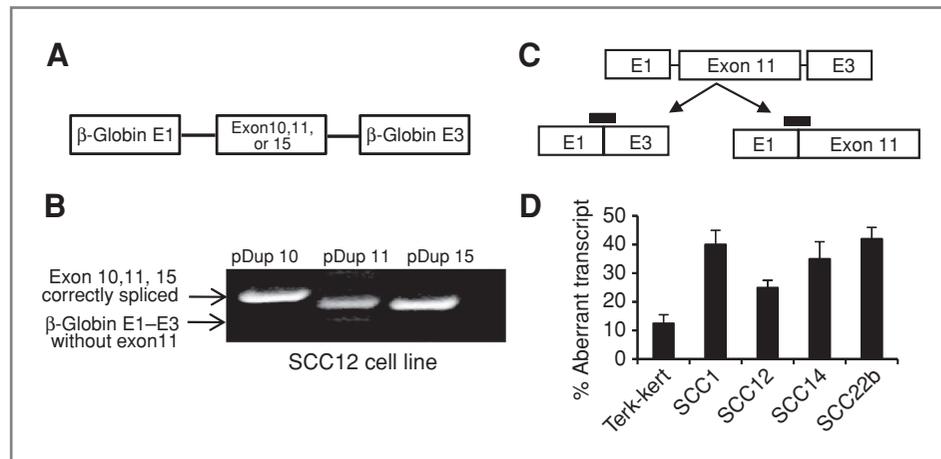


turnover of the aberrant transcript versus wild-type transcripts. UMSCC14 and UMSCC12 head and neck cells were treated with actinomycin D (2 μg/mL) to block transcription and then at different time points, the 2 transcripts were determined by real-time PCR. In both cell lines (Fig. 2B and C), the wild-type E-cadherin transcript was stable over the 2-hour time course whereas the signal from the exon 11–skipped transcript was rapidly lost ($t_{1/2}$ approx 60 minutes), indicating, as expected, its short half-life in head and neck lines. With this short half-life of the exon 11–skipped transcript, our assays on tissues and cells with active NMD pathway underestimate the amount of this transcript.

## Quantification of wild-type and exon 11–skipped transcript

To determine the relative abundance of this aberrant transcript, the head and neck cell lines were analyzed by real-time PCR analysis by using the transcript-specific PCR approach shown in Fig. 1. Figure 2D shows the relative (adjusted to actin) E-cadherin expression in the cell lines compared with 2 normal nontransformed counterparts, NHOK and tert-kert cells. Except for the Cal27 cell line, all the other cell lines have lower E-cadherin levels as compared with the 2 normal nontransformed control cells. Also the relative abundance of exon 11–skipped transcript in the tumorigenic cell lines was higher than in the tert-kert cells (4- to 24-fold higher in 4 of the 6 head and neck cancer cell lines; Fig. 2E). A similar experiment was done on the head and neck cancer cell lines and tert-kert cells treated with emetine (Fig. 2F), in which the percentage of aberrant E-cadherin transcripts was 3- to 8-fold higher in all the head and neck cell lines than tert-kert cells. Thus, exon 11 skipping occurs at a low level in nontransformed oral epithelial cells but is markedly increased in malignant head and neck epithelial tissues.

## Minigene constructs

Exon 11 along with its intronic regions were amplified and sequenced from UMSCC12 and UMSCC22b cells,

and no mutations were identified. This was not unexpected, because as described above, the aberrant splicing was also seen but quantitatively less in normal cells. To further study the mechanism of aberrant splicing and to investigate why it is significantly increased in malignant tissue, exon 11 along with its intronic regions were cloned into the pDup minigene construct (27). As controls, we also cloned E-cadherin exon 10 and 15. The cloned exons were flanked by β-globin, exons E1 and E3 (Fig. 3A). Transfection of the plasmid constructs into UMSCC12 cells and RT-PCR analysis revealed that there is a correctly spliced product (upper band) in cells transfected with exon 10 and 15 pDup constructs. In the case of pDup exon 11 construct, an additional smaller band was seen that lacked exon 11 on sequencing. A transcript-specific real-time PCR strategy similar to the above described E-cadherin wild-type and aberrant transcripts (Fig. 2) was developed to quantify improperly spliced E1–E3 and the correctly spliced E1–exon 11–E3 transcripts in the minigene construct (Fig. 3C). Tert-kert cells and head and neck cell lines were transiently transfected with the exon 11 minigene construct and 48 hours later, a real-time RT-PCR analysis was done. Figure 3D shows head and neck cell lines with a 2- to 3-fold increase in aberrant splicing versus nontransformed tert keratinocytes, providing additional evidence that the E-cadherin exon 11 is improperly spliced in head and neck cell lines.
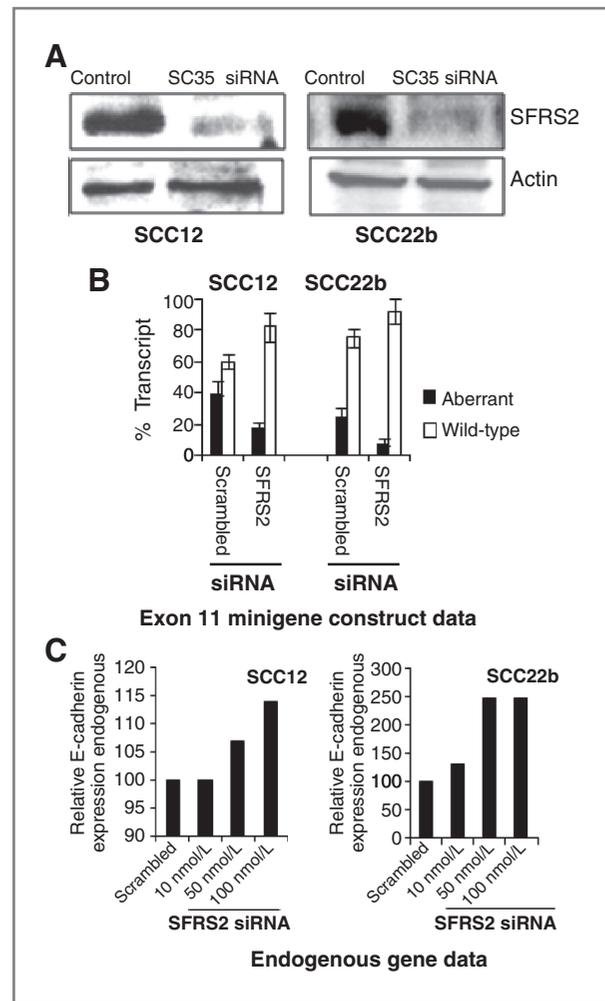
## Role of splicing factors in aberrant splicing

Because we did not identify mutations in exon 11 and the intronic region in 2 head and neck cell lines, we analyzed splicing factors as potential modulators of exon 11 skipping. We analyzed the exon 11 sequence with the exonic splicing enhancer finder software program (33) to determine the putative binding sites of known splicing factors and observed binding sites for the SFRS1, 2, 5, and 6 splice factors (34, 35) in exon 11 and its neighboring intronic region (−225 to +175 bp; Fig. 4). The expression of these splicing factors in head and neck lines relative to
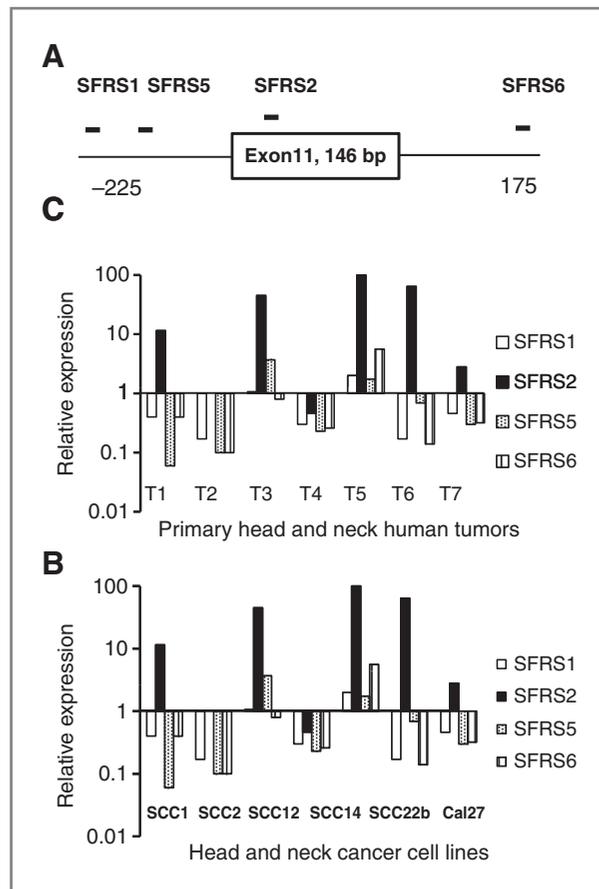
**Figure 4.** Role of splicing factors in aberrant splicing. A, schematic with predicted binding sites for splicing factors around E-cadherin exon 11. B, real-time PCR data for expression of SFRS1, 2, 5, and 6 splicing factors in cell lines relative to tert-kert cells. C, expression of splicing factors by real-time PCR in primary human head and neck tumors relative to matched normal tissue (7 matched pairs).



**Figure 5.** Effect of siRNA-mediated inactivation of SFRS2 on splicing. A, Western blot analysis for UMSCC12 and UMSCC22b cells transfected with SFRS2 siRNA or scrambled control sequence. B, bar diagram with percentage of aberrantly spliced transcript in cells transfected with exon 11 minigene construct and SFRS2 siRNA as determined by transcript-specific real-time PCR in UMSCC12 and UMSCC22b. Control cells were transfected with the exon 11 minigene construct and scrambled siRNA. Data are mean $\pm$ SD, $n = 3$. C, E-cadherin expression by real-time PCR analysis in 2 cell lines transfected with varying amounts of SFRS2 siRNA.

tert-kert is shown in Fig. 4B. A consistent finding was the upregulation of a SFRS2 splicing factor, which formed the rationale for further analysis. Similar analysis in Fig. 4C shows expression of splicing factors in primary head and neck tumors relative to the matched normal tissue. In 5 of 7 pairs analyzed, SFRS2 was also upregulated in tumor tissues as compared with the other splicing factors, which corroborates the head and neck cell line data.

This was further analyzed with the minigene exon 11 construct (Fig. 3A), which was cotransfected with siRNA (10 nmol/L) targeting the splice factor SFRS2 (12) in UMSCC12 and UMSCC22b cells. A scrambled siRNA control transfected along with the minigene construct was used as the control to determine the relative ratio of the correctly spliced E1–11–E3 transcript. Western blot analysis (Fig. 5A) confirmed successful knockdown of SFRS2 in UMSCC12 and UMSCC22b cells. Figure 5B shows the data from 3 transfections (mean $\pm$ SD). In UMSCC12 cells, knockdown of SFRS2 resulted in decrease in aberrant transcript from 40% $\pm$ 8% to 18% $\pm$ 3.6% (mean $\pm$ SD, 2-tailed $P = 0.012$) and in UMSCC22b

cells, the aberrant transcript decreased from 25% $\pm$ 6% to 8% $\pm$ 3.4% (mean $\pm$ SD, 2-tailed $P = 0.013$). Both cell lines showed that inactivation of SFRS2 splicing factor results in an increase in the correctly spliced exon 11 minigene transcript and decrease in the aberrant transcript. To determine the effect of siRNA knockdown on the endogenous E-cadherin gene splicing, these 2 cell lines were transiently transfected with varying amounts (10, 50, and 100 nmol/L) of SFRS2 siRNA (Fig. 5C) and analyzed for RNA transcripts. We observed an increase in wild-type E-cadherin RNA when cells were transfected with increasing amounts of siRNA. The increase in UMSCC12 cells was marginal, whereas in UMSCC22b cells, there was a 2.5-fold increase in wild-type transcripts.

## Methylation status and splicing

Promoter methylation of the E-cadherin gene downregulates its expression (22, 23, 28) that can be reversed by hypomethylating agents, such as azacytidine, which are also being used in the clinical setting as well (reviewed in ref. 36). Also, as transcription and splicing occur simultaneously in the cell and inclusion of certain exons is dependent upon the transcriptional state of the gene, we investigated whether changes in E-cadherin transcription by hypomethylation could affect exon 11 splicing. Two head and neck cancer cell lines, UMSCC1 and 22b, were treated with 5-aza-deoxycytidine (5 μmol/L for 4 days) and analyzed for DNA hypomethylation, E-cadherin expression, and quantification of the 2 transcripts. Figure 6A shows the methylation-specific PCR conducted on bisulfite-treated DNA from untreated and azacytidine-treated cells (28). As expected, azacytidine treatment resulted in the amplification of a band with primers specific for the nonmethylated DNA, which is not seen in DNA from untreated cells. Identically, treated cells also showed increase in E-cadherin expression by Western blot analysis in the 2 cell lines (Fig. 6B). Figures 6C and D describe the RNA transcript analysis with data. UMSCC1 and UMSCC22b cells upon azacytidine treatment showed an increase in the wild-type E-cadherin transcript (16- to 28-fold) with a corresponding decrease in the exon 11–skipped transcript decreases relative to the wild-type transcript (5- to 30-fold decrease). As the overall transcription increases secondary to promoter hypomethylation, it is expected that both the transcripts would increase and potentially increase to the same extent. However the results pointed toward a preferential increase in the wild-type transcript in the azacytidine-treated cells. The data showed that the exon 11–skipped transcript can be clearly modulated by the hypomethylation process and is not a random phenomenon.

## Discussion

We initiated this study to determine whether a previously identified E-cadherin RNA splicing abnormality that results in loss of E-cadherin expression in chronic lymphocytic leukemia cells (21) could also be found in solid tumors. Because the majority of human cancers are epithelial in origin and E-cadherin has a well-documented role in cell–cell adhesion and junctional complexes, we thought it important to see whether exon 11 skipping could play a role in loss of expression. The results show an increase in exon 11–skipped transcript in several solid tumor types along with decreased total E-cadherin expression. Because the frequency of exon 11 skipping was highest in head and neck tumors, we focused on this tumor for subsequent studies. Even though the exon 11–skipped transcript can be amplified from normal control tissues, it is more abundantly expressed in head and neck tumors and cell lines that have a lower expression of E-cadherin.

The differential splicing or changes in alternative splicing patterns of exon 11 between normal and tumor cells could be secondary to differential expression of splicing factors. We chose to study the SFRS2 splicing factor because it has a putative binding site in the E-cadherin exon 11 and is overexpressed in head and neck cell lines and primary tumor tissues as compared with the other splicing factors (Fig. 4, Fig. 5). This splicing factor is reported to have a role in the alternative splicing of the tumor suppressor gene *KLF6* (12). To determine whether the overexpression of this factor plays a role in aberrant splicing, it was knocked down in 2 cell lines and changes in minigene construct splicing pattern were observed (Fig. 5) along with a dose-dependent increase in wild-type E-cadherin expression when different amounts of SFRS2 siRNA were used. The ability of SFRS2 siRNA to significantly enhance exon 11–incorporated transcripts suggests the upregulation of SFRS2 in head and neck cell lines may be involved in aberrant exon 11 splicing. In addition, the ability of knockdown to significantly increase expression of the wild-type transcript in the UMSCC22b cell line suggests that the enhanced aberrant splicing plays a role in loss-of-expression of this tumor suppressor gene rather than just representing an epi-phenomenon. However, it is certainly possible that



**Figure 6.** Hypomethylating agent and aberrant splicing. A, methylation-specific PCR for UMSCC1 and UMSCC22b cell lines with and without azacytidine treatment. B, Western blot analysis for UMSCC1 and UMSCC22b showing E-cadherin expression and actin control with azacytidine treatment. C, expression of wild-type E-cadherin transcripts relative to the untreated cells and adjusted to actin, along with the percentage of aberrant transcript after azacytidine treatment.
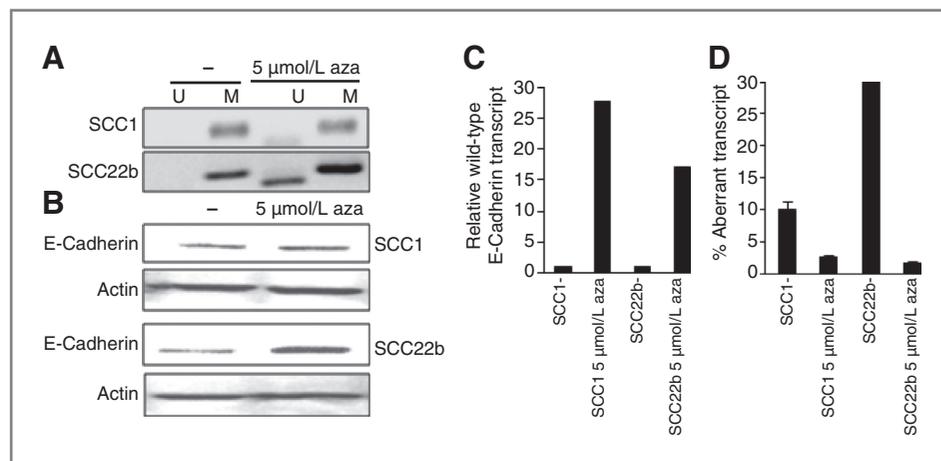
additional splicing factors not studied also play a role in the observed aberrant splicing.

Our studies with azacytidine address 2 related processes, gene transcription and splicing. Our data show that azacytidine treatment results in hypomethylation of the E-cadherin promoter and an increase in transcription (Fig. 6), along with changes in the splicing pattern of the cells with a preferential increase in the wild-type transcript. Conversely, methylation of this gene that is frequently observed in human malignancies can potentially decrease E-cadherin expression with both transcriptional repression and an increase in exon 11 missplicing. There are 2 possible explanations for methylation status to result in splicing changes. First, hypomethylation changes the nature of the transcriptional complex formed at the promoter that then recruits additional factors that have a dual role as transcriptional factors and also affect splicing of exons (37–40). In the fibronectin gene model, the C-terminal domain is required for interaction with inhibitory splicing factors such as SRp20 to promote exon skipping (17). Second, methylation could influence the lysine residues of the histones (reviewed in 14, 18, 36, 41) and the resulting chromatin changes increase exon 11 missplicing, which is reversed by azacytidine treatment. Studies are ongoing to further elucidate the relative contribution of these 2 processes in exon 11 skipping.

In summary, head and neck cancer cell lines, primary tissues, and a number of other malignancies harbor an aberrantly spliced E-cadherin transcript that is present in much larger amounts as compared with the normal cells. As expression of *E-cadherin gene* is frequently lost in tumor cells, missplicing of this exon is an interesting model to study the potential role of genetic and epigenetic events that affect splicing in cancer cells. It is also plausible that transcription factors involved in epithelial to mesenchymal transformation, for example, snail and zeb (42, 43), change the splicing milieu of the cells as they downregulate E-cadherin expression. The findings have a potential for clinical implications as epigenetic events can be reversed for reexpressing this tumor suppressor gene.

## Disclosure of Potential Conflicts of Interest

No potential conflicts of interest were disclosed.

## References

1. Chang YF, Imam JS, Wilkinson MF. The nonsense-mediated decay RNA surveillance pathway. Annu Rev Biochem 2007;76: 51–74.
2. Culbertson MR. RNA surveillance. Unforeseen consequences for gene expression, inherited genetic disorders and cancer. Trends Genet 1999;15:74–80.
3. Frischmeyer PA, van Hoof A, O'Donnell K, Guerrerio AL, Parker R, Dietz HC. An mRNA surveillance mechanism that eliminates transcripts lacking termination codons. Science 2002;295: 2258–61.
4. Lander ES, Linton LM, Birren B, Nusbaum C, Zody MC, Baldwin J,, et al. Initial sequencing and analysis of the human genome. Nature 2001;409:860–921.
5. Venables JP. Unbalanced alternative splicing and its significance in cancer. Bioessays 2006;28:378–86.
6. Couch FJ, Weber BL. Mutations and polymorphisms in the familial early-onset breast cancer (BRCA1) gene. Breast Cancer Information Core. Hum Mutat 1996;8:8–18.
7. El-Bchiri J, Buhard O, Penard-Lacronique V, Thomas G, Hamelin R, Duval A. Differential nonsense mediated decay of mutated mRNAs in mismatch repair deficient colorectal cancers. Hum Mol Genet 2005;14:2435–42.
8. Abbas S, Erpelinck-Verschueren CA, Goudswaard CS, Lowenberg B, Valk PJ. Mutant Wilms' tumor 1 (WT1) mRNA with premature termination codons in acute myeloid leukemia (AML) is sensitive to nonsense-mediated RNA decay (NMD). Leukemia 2009;24:660–3.
9. Bartel F, Taubert H, Harris LC. Alternative and aberrant splicing of MDM2 mRNA in human cancer. Cancer Cell 2002;2:9–15.
10. Gilad S, Khosravi R, Shkedy D, Uziel T, Ziv Y, Savitsky K, et al. Predominance of null mutations in ataxia-telangiectasia. Hum Mol Genet 1996;5:433–9.
11. Karni R, de Stanchina E, Lowe SW, Sinha R, Mu D, Krainer AR. The gene encoding the splicing factor SF2/ASF is a proto-oncogene. Nat Struct Mol Biol 2007;14:185–93.
12. Shi J, Hu Z, Pabon K, Scotto KW. Caffeine regulates alternative splicing in a subset of cancer-associated genes: a role for SC35. Mol Cell Biol 2008;28:883–95.
13. Eisenreich A, Malz R, Pepke W, Ayral Y, Poller W, Schultheiss HP, et al. Role of the phosphatidylinositol 3-kinase/protein kinase B pathway in regulating alternative splicing of tissue factor mRNA in human endothelial cells. Circ J 2009;73:1746–52.
14. Sharma S, Kelly TK, Jones PA. Epigenetics in cancer. Carcinogenesis 2010;31:27–36.
15. Kornblihtt AR. Chromatin, transcript elongation and alternative splicing. Nat Struct Mol Biol 2006;13:5–7.
16. Kornblihtt AR. Coupling transcription and alternative splicing. Adv Exp Med Biol 2007;623:175–89.
17. de la Mata M, Kornblihtt AR. RNA polymerase II C-terminal domain mediates regulation of alternative splicing by SRp20. Nat Struct Mol Biol 2006;13:973–80.
18. Schwartz S, Ast G. Chromatin density and splicing destiny: on the cross-talk between chromatin structure and splicing. EMBO J 2010;29:1629–36.
19. Luco RF, Pan Q, Tominaga K, Blencowe BJ, Pereira-Smith OM, Misteli T. Regulation of alternative splicing by histone modifications. Science 2010;327:996–1000.

20. Schwartz S, Meshorer E, Ast G. Chromatin organization marks exon-intron structure. Nat Struct Mol Biol 2009;16:990–5.

21. Sharma S, Lichtenstein A. Aberrant splicing of the E-cadherin transcript is a novel mechanism of gene silencing in chronic lymphocytic leukemia cells. Blood 2009;114:4179–85.

22. Jeanes A, Gottardi CJ, Yap AS. Cadherins and cancer: how does cadherin dysfunction promote tumor progression? Oncogene 2008; 27:6920–9.

23. Pecina-Slaus N. Tumor suppressor gene E-cadherin and its role in normal and malignant cells. Cancer Cell Int 2003;3:17.

24. Pfaffl MW. A new mathematical model for relative quantification in real-time RT-PCR. Nucleic Acids Res 2001;29:e45.

25. Park NH, Min BM, Li SL, Huang MZ, Cherick HM, Doniger J. Immortalization of normal human oral keratinocytes with type 16 human papillomavirus. Carcinogenesis 1991;12:1627–31.

26. Noensie EN, Dietz HC. A strategy for disease gene identification through nonsense-mediated mRNA decay inhibition. Nat Biotechnol 2001;19:434–9.

27. Modafferi EF, Black DL. A complex intronic splicing enhancer from the c-src pre-mRNA activates inclusion of a heterologous exon. Mol Cell Biol 1997;17:6537–45.

28. Nakayama S, Sasaki A, Mese H, Alcalde RE, Tsuji T, Matsumura T. The E-cadherin gene is silenced by CpG methylation in human oral squamous cell carcinomas. Int J Cancer 2001;93:667–73.

29. Gervais ML, Henry PC, Saravanan A, Burry TN, Gallie BL, Jewett MA, et al. Nuclear E-cadherin and VHL immunoreactivity are prognostic indicators of clear-cell renal cell carcinoma. Lab Invest 2007;87:1252–64.

30. Endo K, Ueda T, Ueyama J, Ohta T, Terada T. Immunoreactive E-cadherin, alpha-catenin, beta-catenin, and gamma-catenin proteins in hepatocellular carcinoma: relationships with tumor grade, clinico-pathologic parameters, and patients' survival. Hum Pathol 2000;31: 558–65.

31. Kurtz KA, Hoffman HT, Zimmerman MB, Robinson RA. Decreased E-cadherin but not beta-catenin expression is associated with vascular invasion and decreased survival in head and neck squamous carcinomas. Otolaryngol Head Neck Surg 2006;134:142–6.

32. Ionov Y, Nowak N, Perucho M, Markowitz S, Cowell JK. Manipulation of nonsense mediated decay identifies gene mutations in colon cancer Cells with microsatellite instability. Oncogene 2004;23: 639–45.

33. Cartegni L, Wang J, Zhu Z, Zhang MQ, Krainer AR. ESEfinder: A web resource to identify exonic splicing enhancers. Nucleic Acids Res 2003;31:3568–71.

34. Ghosh G, Adams JA. Phosphorylation mechanism and structure of serine-arginine protein kinases. FEBS J 2011;278:587–97.

35. Lin S, Fu XD. SR proteins and related factors in alternative splicing. Adv Exp Med Biol 2007;623:107–22.

36. Yang X, Lay F, Han H, Jones PA. Targeting DNA methylation for epigenetic therapy. Trends Pharmacol Sci 2010;31:536–46.

37. Luco RF, Allo M, Schor IE, Kornblihtt AR, Misteli T. Epigenetics in alternative pre-mRNA splicing. Cell 2011;144:16–26.

38. Munoz MJ, de la Mata M, Kornblihtt AR. The carboxy terminal domain of RNA polymerase II and alternative splicing. Trends Biochem Sci 2010;35:497–504.

39. Kornblihtt AR. Promoter usage and alternative splicing. Curr Opin Cell Biol 2005;17:262–8.

40. Perales R, Bentley D. "Cotranscriptionality": the transcription elongation complex as a nexus for nuclear transactions. Mol Cell 2009;36:178–91.

41. Kolasinska-Zwierz P, Down T, Latorre I, Liu T, Liu XS, Ahringer J. Differential chromatin marking of introns and expressed exons by H3K36me3. Nat Genet 2009;41:376–81.

42. Peinado H, Olmeda D, Cano A. Snail, Zeb and bHLH factors in tumour progression: an alliance against the epithelial phenotype? Nat Rev Cancer 2007;7:415–28.

43. Mani SA, Guo W, Liao MJ, Eaton EN, Ayyanan A, Zhou AY,, et al. The epithelial-mesenchymal transition generates cells with properties of stem cells. Cell 2008;133:704–15.

AAC-R American Association for Cancer Research

# Molecular Cancer Therapeutics

# Exon 11 Skipping of E-Cadherin RNA Downregulates Its Expression in Head and Neck Cancer Cells

Sanjai Sharma, Wei Liao, Xiaofeng Zhou, et al.

| | |
|---|---|
| **Updated version** | Access the most recent version of this article at:<br>doi:10.1158/1535-7163.MCT-11-0248 |
| **Supplementary Material** | Access the most recent supplemental material at:<br>http://mct.aacrjournals.org/content/suppl/2011/07/13/1535-7163.MCT-11-0248.DC1 |

| | |
|---|---|
| **Cited articles** | This article cites 43 articles, 5 of which you can access for free at:<br>http://mct.aacrjournals.org/content/10/9/1751.full#ref-list-1 |

| | |
|---|---|
| **E-mail alerts** | Sign up to receive free email-alerts related to this article or journal. |
| **Reprints and Subscriptions** | To order reprints of this article or to subscribe to the journal, contact the AACR Publications Department at pubs@aacr.org. |
| **Permissions** | To request permission to re-use all or part of this article, use this link<br>http://mct.aacrjournals.org/content/10/9/1751.<br>Click on "Request Permissions" which will take you to the Copyright Clearance Center's (CCC)<br>Rightslink site. |